

JGR Space Physics



RESEARCH ARTICLE

10.1029/2023JA031445

Key Points:

- Recurrent magnetic dipolarization and Energetic Neutral Atoms (ENA) enhancement are correlated
- The SKR and 20 kHz narrow band emissions are likely connected to the rotating hot plasma cloud revealed by ENA observation
- Periodic enhancements of SKR are concurrent but slightly time-lag/lead the recurrent magnetic dipolarizations

Supporting Information:

Supporting Information may be found in the online version of this article.

Correspondence to:













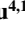



Z. H. Yao,
z.yao@ucl.ac.uk

Citation:

Xu, Y., Yao, Z. H., Ye, S.-Y., Badman, S. V., Dialynas, K., Sergis, N., et al. (2023). A possible unified picture for the connected recurrent magnetic dipolarization, quasi-periodic ENA enhancement, SKR low-frequency extension and narrowband emission at Saturn. *Journal of Geophysical Research: Space Physics*, 128, e2023JA031445. <https://doi.org/10.1029/2023JA031445>

Received 27 FEB 2023
Accepted 8 AUG 2023

A Possible Unified Picture for the Connected Recurrent Magnetic Dipolarization, Quasi-Periodic ENA Enhancement, SKR Low-Frequency Extension and Narrowband Emission at Saturn

Y. Xu^{1,2} , Z. H. Yao^{1,2,3} , S.-Y. Ye⁴, S. V. Badman⁵ , K. Dialynas⁶ , N. Sergis^{6,7} , L. C. Ray⁵ , R. L. Guo⁸ , D. X. Pan⁹ , W. R. Dunn³ , B. Zhang¹⁰ , A. Bader¹¹ , J. Kinrade⁵ , S. Y. Wu^{4,12} , A. J. Coates³ , D. G. Mitchell¹³ , and Y. Wei^{1,2} 

¹Key Laboratory of Earth and Planetary Physics, Institute of Geology and Geophysics, Chinese Academy of Sciences, Beijing, China, ²College of Earth and Planetary Sciences, University of Chinese Academy of Sciences, Beijing, China, ³UCL Mullard Space Science Laboratory, Dorking, UK, ⁴Department of Earth and Space Sciences, Southern University of Science and Technology (SUSTech), Shenzhen, China, ⁵Department of Physics, Lancaster University, Lancaster, UK, ⁶Office of Space Research and Technology, Academy of Athens, Athens, Greece, ⁷National Observatory of Athens, Institute of Astronomy, Astrophysics, Space Applications and Remote Sensing, Athens, Greece, ⁸Laboratory of Optical Astronomy and Solar-Terrestrial Environment, School of Space Science and Physics, Institute of Space Sciences, Shandong University, Weihai, China, ⁹School of Geophysics and Information Technology, China University of Geosciences (Beijing), Beijing, China, ¹⁰Department of Earth Sciences, the University of Hong Kong, Pokfulam, China, ¹¹Gorilla, Antwerp, Belgium, ¹²LESIA, Observatoire de Paris, Université PSL, CNRS, Sorbonne Université, Université de Paris, Paris, France, ¹³Johns Hopkins University Applied Physics Laboratory, Laurel, MD, USA

Abstract Magnetic Dipolarization, a hallmark indicator of the formation of field-aligned currents, plays a crucial role in the energy dissipative processes that occur within planetary magnetospheres. Saturn's magnetic dipolarization was found to recur after one planetary rotation, suggesting a potential correlation with the corotating current systems. The observation of enhanced Energetic Neutral Atoms (ENA) within Saturn's inner magnetosphere serves as a diagnostic tool, revealing the existence of a rotating, dynamic Partial Ring Current (PRC) system. By utilizing multiple datasets from Cassini, this study advances the understanding of the interrelationship between ENA emission and magnetic dipolarization. Our results suggest the possibility of a coupling between the PRC system revealed by the ENA emission and magnetic dipolarization. Furthermore, a temporal correlation was found between the ENA emissions and two distinct radio emissions. This study discusses potential causal relationships among these phenomena and first time proposes a global unified physical picture.

Plain Language Summary Energy dissipation and circulation are the core of the space plasma field, which shows different typical features at different planets. Unlike the solar wind-driven terrestrial magnetosphere, the giant planetary magnetospheric processes are strongly controlled by internal processes, and show strong rotational modulation in the in situ and remote sensing measurements. The rotation modulation of the observations in Saturn's magnetosphere may lead to challenges in the interpretation of data. The observed variations in data are a combination of spatial and temporal variations. In this study, we analyzed the multiple datasets from Cassini to formulate a uniform picture of the periodic variations including magnetic field variation, rotating hot plasma cloud, and radio emissions. We propose that the corotating current system could potentially connect all observed phenomena.

1. Introduction

Saturn's ionosphere and atmosphere are coupled with the magnetosphere through magnetic field lines, allowing exchanges of mass and energy (Brooks et al., 2019; Bunce et al., 2008; Mitchell, Krimigis, et al., 2009; Mitchell, Kurth et al., 2009; Palmaerts et al., 2020; Schippers et al., 2012; Wing et al., 2020; Yao, 2017; Yao, Coates, et al., 2017). Solar wind and planetary internal sources jointly drive the dynamic processes in Saturn's magnetosphere (e.g., see a brief overview in Dialynas, 2018), leading to the reconfiguration of magnetospheric field lines via changing electrical current systems (e.g., Brandt et al., 2010; Bradley et al., 2018). Due to the rapid planetary rotation and the heavy mass-loading source of Saturn's inner moon Enceladus that supplies the system with copious amounts of water group plasma (Dougherty et al., 2006; Smith et al., 2010), Saturn's magnetic field near

© 2023. The Authors.

This is an open access article under the terms of the [Creative Commons Attribution License](https://creativecommons.org/licenses/by/4.0/), which permits use, distribution and reproduction in any medium, provided the original work is properly cited.

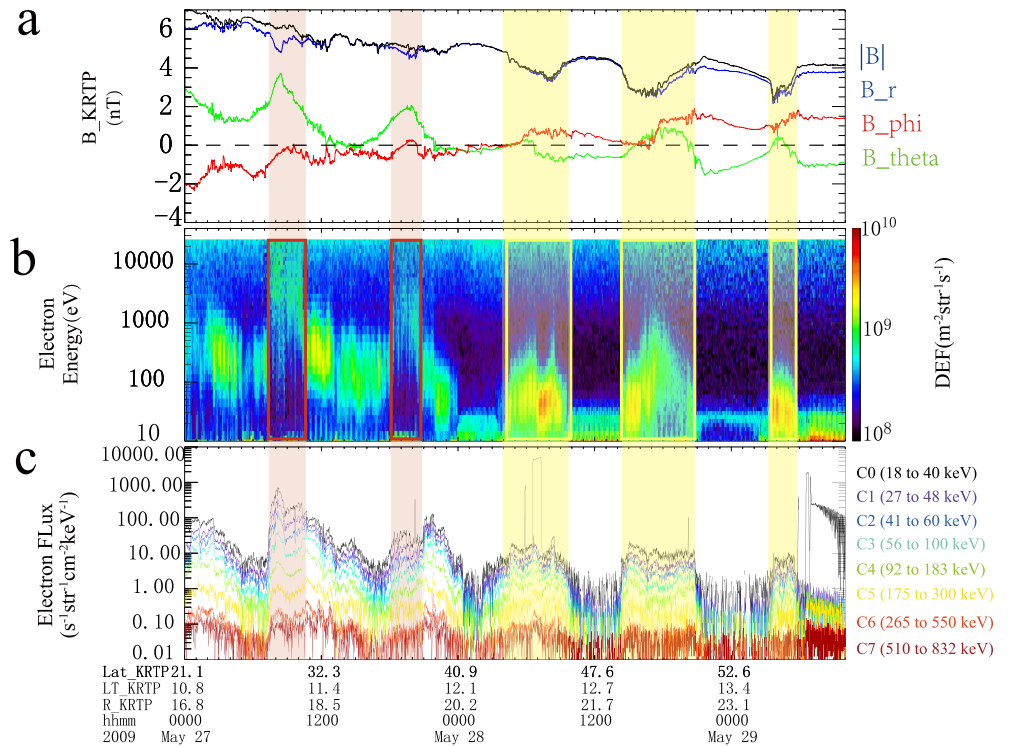


Figure 1. Recurrent magnetic signals from May 27th 00:00 to May 29th 10:00, 2009. (a) Total magnetic field magnitude and three magnetic field components in KRTP (Kronocentric-R-Theta-Phi) coordinates, which is a Kronocentric spherical coordinate. “R” is the radial distance, “Theta” is the polar angle and “Phi” is the azimuth angle. (b) Energy spectrogram of omnidirectional electron flux from CAPS-ELS. (c) Differential flux of energetic electrons from MIMI-LEMMS. The red shadings represent recurrent magnetic dipolarization structures. The yellow shadings are regions where Cassini encountered the cusp. The start and end times of all recurrent magnetic signals are collated in Table 1.

the equator is usually highly stretched to form a magnetodisc (Achilleos et al., 2010; Arridge et al., 2008), and creates an intense azimuthal current in Saturn's plasmasphere (Krimigis et al., 2007; Sergis et al., 2007). Processes that rapidly release energy often occur in Saturn's magnetosphere and are associated with the current diversion into the ionosphere, forming a current wedge and resulting in magnetic dipolarization signatures. The rapid energy release could accelerate charged particles, causing particle precipitation into the ionosphere and upper atmosphere of Saturn (Kivelson, 2005), to enhance the polar auroral emission. Yao et al. (2018) reported the recurrent nature of magnetic dipolarization at Saturn and suggested that the dipolarized magnetic field lines may corotate with the planet. They also proposed that magnetic dipolarization, auroral emission and the enhancement of the ENA emission are connected processes in the magnetosphere-ionosphere coupling system. Due to the high variability of the auroral morphology and magnetospheric dynamics, the relation between auroral dynamics and magnetospheric dynamics is yet to be understood.

The energetic neutral atoms (ENA), which are produced by charge-exchange collisions between residual neutral particles and trapped energetic ions in Saturn's magnetosphere, were imaged by the Cassini/Ion and Neutral Camera (INCA) to provide a visualization of the Kronian non-axisymmetric Partial Ring Current (PRC) system (Brandt et al., 2010; Carbary, Mitchell, Brandt, Roelof, & Krimigis, 2008; Carbary & Mitchell, 2014; Krimigis et al., 2007; Sergis et al., 2017). INCA, part of the Magnetospheric Imaging Instrument (MIMI; Krimigis et al., 2004) suite on Cassini was a large geometry factor ($G \sim 0.6 \text{ cm}^2 \text{ sr}$ for H) camera that can separate and identify the composition of Hydrogen and Oxygen (H and O), and analyze the direction of the incident ENA, via the time-of-flight (TOF) technique, over the energy range of ~ 5.4 to >220 keV and provided an invaluable tool to remotely capture a global picture of ion acceleration events (Dialynas et al., 2013). The rotational modulation of energetic ions, ENAs and their connections to the quasi-periodic magnetic field perturbations and associated auroral emissions have been the subject of extensive past research (Brandt et al., 2010; Carbary et al., 2007; Krimigis et al., 2005; Mitchell, Krimigis, et al., 2009; Palmaerts et al., 2020). The ENA emissions are found

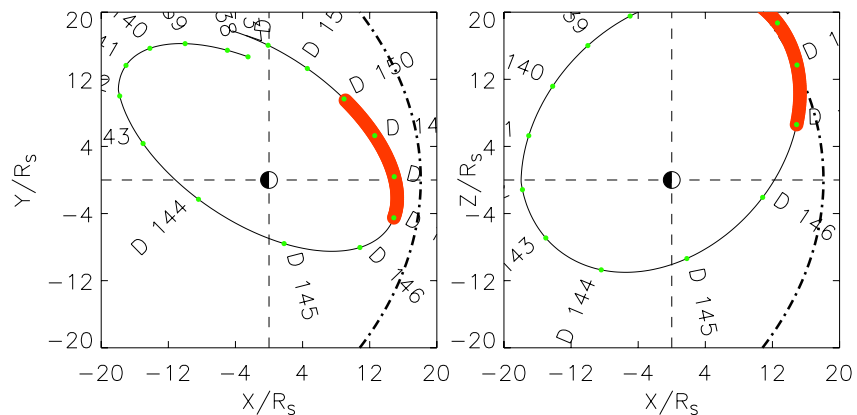


Figure 2. Trajectory of Cassini from May 17 to 3 June 2009 (Rev 111, day 137–150) in Kronocentric Solar Magnetospheric coordinate. (a) The X-Y view; (b) The X-Z view. Event observation periods are highlighted in red (DOY 147–150, May 27 to 30 May 2009).

to rotate at a period of ~ 11 hr, with significant local time modulation (Carbary, Mitchell, Brandt, Paranicas, & Krimigis, 2008; Carbary et al., 2009, 2010). The peak count of the ENA emission (on average) is noted to occur in Saturn's nightside magnetosphere (Bader et al., 2021; Dialynas et al., 2013; Kinrade et al., 2021; Krimigis et al., 2005). Moreover, O emission exhibits a period of 10.8 ± 0.2 hr, while the H emission has more irregular periods (8–13 hr) (Carbary, Mitchell, Brandt, Paranicas, & Krimigis, 2008). Plasma injections have been interpreted as possible triggers of ENA enhancements in Saturn's magnetosphere (Mitchell et al., 2015) and are also shown to have noticeable effects on the energetic ion distributions and their properties (e.g., Dialynas et al., 2018). Moreover, ENA and auroral enhancements are found to be coherent in time and local time (Kinrade et al., 2020; Mitchell, Krimigis, et al., 2009; Palmaerts et al., 2020), indicating that the perturbations of ENA in the magnetosphere are associated with Field-Aligned Current (FAC) formation. Palmaerts et al. (2020) presented an enhanced ENA emission for several successive planetary rotations, which was accompanied by a rotating auroral spiral structure, highlighting the importance of the rotating magnetosphere-ionosphere coupling current system at Saturn.

A close relationship between the recurrent ENA enhancements and bursts of Saturn Kilometric Radiation had been identified using Cassini's datasets (Mitchell, Krimigis, et al., 2009). SKR is a consequence of the magnetosphere-ionosphere coupling processes (Lamy et al., 2018). The electron cyclotron maser instability, excited by auroral precipitating electrons with loss cone distributions, is the prevalent generation mechanism of SKR (Lamy et al., 2010; Wu & Lee, 1979). SKR has frequencies ranging from ~ 10 to $\sim 1,500$ kHz (Lamy et al., 2008; Kurth et al., 2009). The auroral kilometric radiation is a fundamental phenomenon associated with planetary auroral processes, and has often been observed at the Earth (Gurnett, 1974) and Jupiter (Green & Boardsen, 1999; Kurth et al., 1980, 2005; Morgan & Gurnett, 1991), and other magnetized planets (Zarka, 1998 and references therein). At lower frequencies, the Saturnian magnetosphere emits numerous radio emissions. Apart from the SKR emission, narrow band (NB) emissions are often observed (Gurnett et al., 1981). NB emissions are detected at around ~ 5 and ~ 20 kHz (Ye et al., 2009), and usually appear periodically within a few days after the enhancement of SKR. Ye et al. (2009) also found that the source region of the 20 kHz NB emissions is consistent with the model proposed by Jones (1976) and Melrose (1981), where the electrostatic upper hybrid waves on the boundary of the plasma torus mode convert to the L-O mode. However, the 5 kHz NB's source location obtained by goniopolarimetric analysis is not consistent with the model prediction, suggesting that the 5 kHz NB may be associated with a different source and driving mechanisms. Furthermore, Ye et al. (2009) showed that 20 kHz NB emissions originate from the northern and southern edges of Saturn's plasma torus at $L \sim 4$ to 7, which is rather close to the source region of ENA (e.g., Bader et al., 2021; Kinrade et al., 2021). Wing et al. (2020) suggested that the 5 kHz NB emission may be related to the ENA brightening events. Whether the ENA emission is related to 20 kHz NB is still poorly understood.

Previous studies have established correlations among a portion of these processes/phenomena, but there is still a lack of a global unified physical picture. In this study, we use simultaneous unprecedented observations

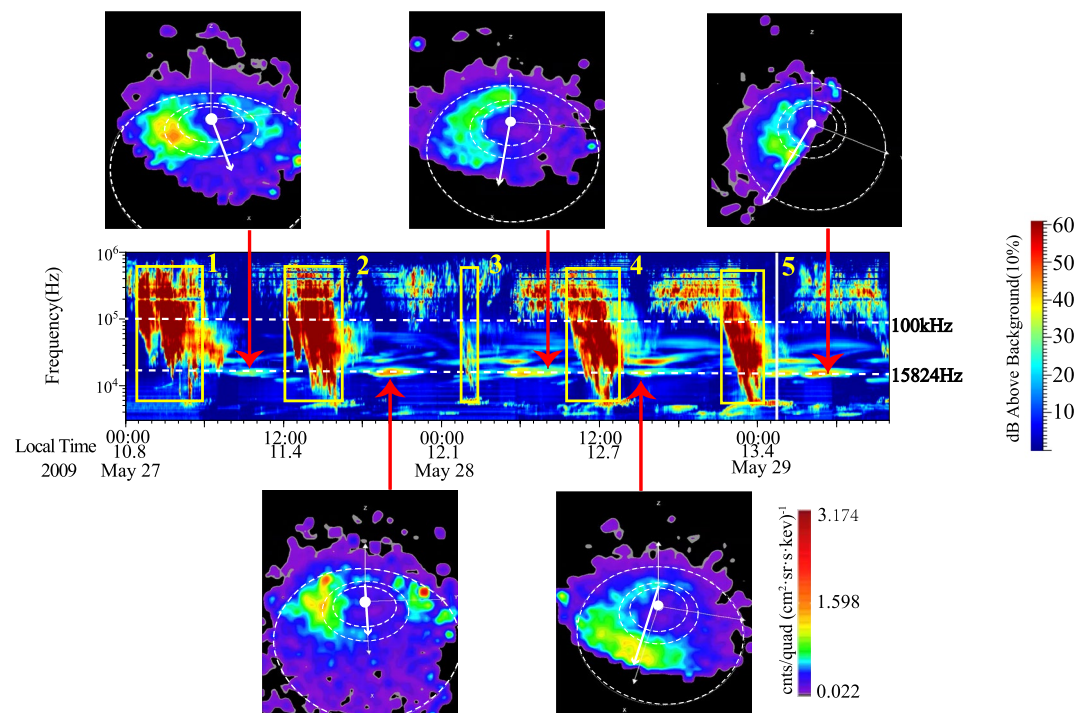


Figure 3. Evidence of the close relationship among the brightened Energetic Neutral Atoms (ENA) emissions, the enhanced 20 kHz signals and SKR signals from May 27th 00:00 to May 29th 10:00, 2009. The center panel shows the Cassini RPWS electric power with the local time location of the spacecraft shown below, where the yellow rectangle indicates the SKR signal that extends to low frequencies. The enhanced 20 kHz NB signal appears after each SKR enhancement. The colorbar shows the wave intensity in dB above background (set at the 10% level of occurrence). The top and bottom panels show the ENA emission peaks captured during the 20 kHz NB signals and aligned to the center panel by the red arrows according to the time of occurrence. The dotted circles in ENA imaging represent the orbits of Titan at $20R_s$, Rhea at $8.7R_s$, and Dione at $6.25R_s$. The white dotted lines in the center panel represent a cut of the wave intensity at 100 kHz (represents SKR low-frequency extension) 15824 Hz (represent 20 kHz NB), corresponding to Figure 4. The White arrows in ENA images point to the Sun.

obtained from Cassini's INCA, MAG (Magnetometer), RPWS (Radio and Plasma Wave Science) and CAPS (Cassini Plasma Spectrometer) instruments (Jaffe & Herrell, 1997) to present concurrent observations of ENA, magnetic dipolarization, 20 kHz NB, and SKR. And we for the first time, propose a possible physical connection between Saturn's ENA enhancement, magnetic dipolarization, SKR low-frequency extension and 20 kHz NB emission.

2. Observations

The magnetic field observations in Figure 1a are obtained by the Cassini-MAG instrument (Dougherty et al., 2004). The thermal electron measurements (Figure 1b) are from the Cassini-CAPS/ELS (Young et al., 2004), with an energy range of up to 28 keV for electrons. The in situ energetic electron measurements of ~ 18 –832 keV (Figure 1c) come from the Low-Energy Magnetospheric Measurements System, whereas the 24–55 keV ENA images in Figure 3, corresponding to protons of the same energies, are obtained from the INCA of the Magnetosphere Imaging Instrument (MIMI) (Krimigis et al., 2004). The Cassini SKR and NB observations in Figures 3 and 4 are obtained by the High Frequency Receiver of the Radio and Plasma Wave Science (RPWS) instrument (Gurnett et al., 2004).

The observations of recurrent magnetic signals (B_θ rising and B_r falling) over five planetary rotations within the period from May 27th 00:00 to May 29th 10:00, 2009 are presented in Figure 1. The first two features are accompanied by a higher energy electron spectrum (Figure 1b) than the ambient plasma and significantly enhanced electron flux (Figure 1c), indicating particle accelerations associated with these magnetic structures, which may power the polar auroral emissions (Yao et al., 2018). These are typical features of current redistribu-

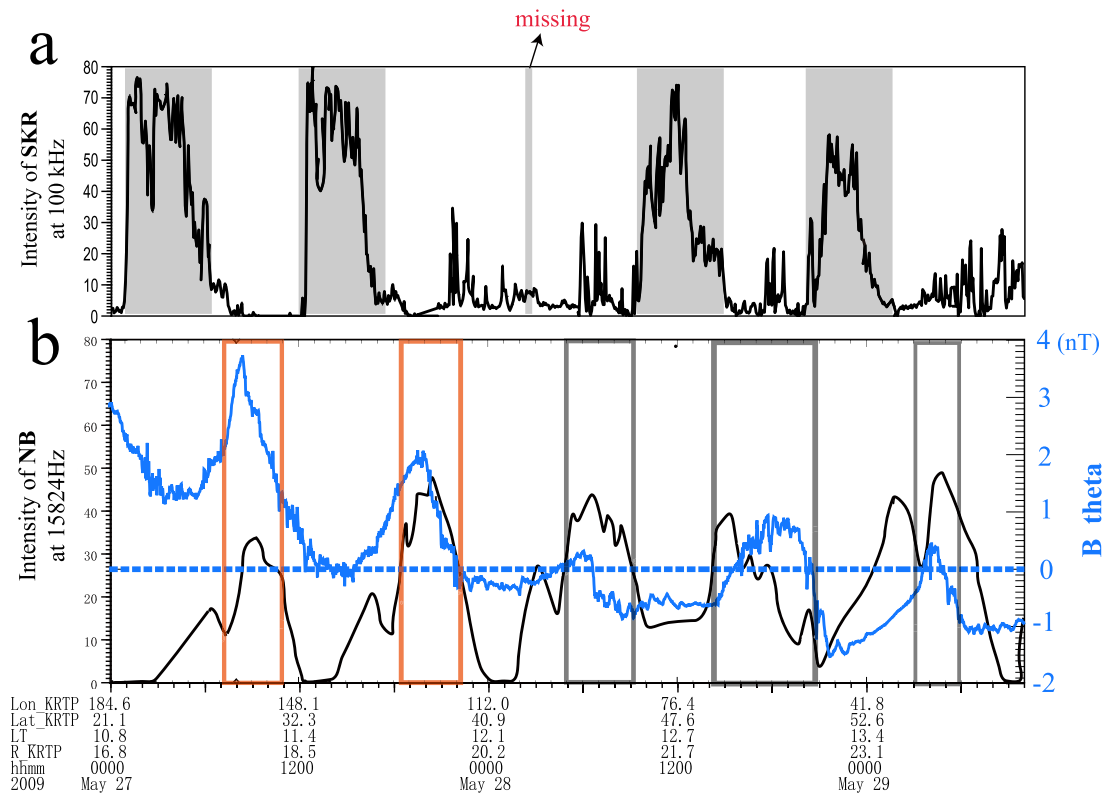


Figure 4. Evidence of the close relationship between the dipolarization signals and the enhanced 20 kHz signals. (a) The variation of the intensity of SKR at 100 kHz (other signals at 100 kHz have been filtered) corresponding to the white dashed line in the center of Figure 3. Gray shading indicates SKR events that are significantly enhanced compared to the background. (b) The variation of intensity of NB at 15824 Hz, while the blue curve shows the B_{θ} component. The rectangles emphasize their correspondence. The red rectangles represent the magnetic dipolarization events and the gray rectangles represent cusp crossing events.

tion dipolarization as described in Yao, Grodent, et al. (2017). So the first two signals were identified as recurrent magnetic dipolarization structures (Yao et al., 2018) on the dayside. Notably, the interval between the dipolarization signals is about one planetary rotation period (~ 11 hr), as a consequence of rotation modulation. After 00:00 on May 28, Cassini entered mid-to-high latitude regions at near-noon local times as Figure 2 presents. As shown in Figure 1, from 4:20 on May 28 to 5:50 on May 29, three recurrent magnetic signals observed at the same cadence afterward were detected accompanied by electrons with low-energy fluxes (10 to hundreds eV) and the electrons have temperatures of 10 \sim 100 eV (see Figure S1 in Supporting Information S1). These plasma features in the yellow-shaded regions are consistent with magnetosheath populations, which are typical signatures of the cusp (Arridge et al., 2016; Jasinski et al., 2014, 2016). In the yellow-shaded regions, the total magnetic field intensity decreases significantly, showing diamagnetic depression in the cusp region (Jasinski et al., 2017). Thus, the last three recurrent magnetic signals were identified as cusp crossing. The separation of three cusp signals is one planetary rotation period (~ 11 hr), suggesting the periodic oscillations of the cusp's location (Arridge et al., 2016). For the other regions, the field strength varied more gently, and the electron fluxes are observed at the instrument noise level, indicating the motion of the spacecraft into the polar cap. From the observational features between 4:20 on May 28 and 5:50 on May 29, we infer that Cassini was swapping between the polar cap and cusp. We notice that there was a strong enhancement of energetic electrons with energies greater than 10 keV 1 day before the reported dipolarization, which is perhaps the source region of the recurrent dipolarization. The details are presented in Figure S2.

Figure 3 shows the frequency-time spectrogram of radio emission and the corresponding ENA images, which have the same time range as Figure 1. In the five successive planetary rotations, five enhanced SKR signals (four strongly enhanced SKR signals and one slightly enhanced SKR signal) over the frequency range of 10–100 kHz are detected every ~ 11 hr (marked by numbered yellow rectangles). Among these signals, the third SKR intensification was mostly missing. The missing signal could be caused by the solar wind compression on Kronian

Table 1

Start/End Time List in May 2009 for Periodic Features in the Observations Including SKR Low-Frequency Extension, Recurrent Magnetic Field Signal (Including Recurrent Dipolarizations and Cusp Magnetic Signals), 20 kHz NB Enhancement and ENA Emission

Observation number	1		2		3		4		5	
	Start	End	Start	End	Start	End	Start	End	Start	End
SKR enhancement	27/00:57	27/06:05	27/12:05	27/16:14	-	-	28/09:40	28/12:57	28/19:10	28/23:45
SKR enhancement +5h	27/05:57	27/11:05	27/17:05	27/21:14	-	-	28/14:40	28/17:57	29/00:10	29/04:45
recurrent magnetic field signal	27/07:14	27/10:32	27/18:00	27/20:35	28/04:18	28/09:40	28/14:31	28/20:55	29/03:19	29/05:50
20 kHz NB enhancement	27/08:15	27/10:37	27/18:30	27/22:04	28/04:57	28/09:10	28/14:02	28/16:04	29/03:08	29/07:00
ENA enhancement	27/09:03	27/09:51	27/19:39	27/20:27	28/07:47	28/08:15	28/14:39	28/15:27	29/05:02	29/05:38

Note. Regarding the SKR enhancement, Table 1 records the start/end times of the 100 kHz low-frequency part enhancement compared to the background, see Figure 4a. The start/end times of the recurrent magnetic signals correspond to the colored shadings in Figure 1. The first two magnetic signals are dipolarization signals observed in the magnetosphere, followed by three cusp magnetic signals observed by Cassini at the same cadence. With regard to the 20 kHz NB enhancement, Table 1 records the start/end times of the 15824 Hz NB enhancement over 27 dB, as shown in the blue dashed line in Figure 4b. The start/end time of the ENA emission corresponds to the duration of ENA image accumulation in Figure 3.

magnetospheres, which may have disturbed the magnetic field, moving the SKR beam away from Cassini. Thus, the spacecraft would be in an inappropriate position to receive SKR signals (Kurth et al., 2005). All other enhanced SKR emissions are identified as extending to low frequencies (10 kHz), suggesting that the auroral particle acceleration region extends to higher altitudes along magnetic field lines (Jackman et al., 2009) and may also indicate intense auroral activity (Kurth et al., 2016; Lamy et al., 2018). All enhanced SKR emissions are right-hand polarized as would be expected for emissions from the northern hemisphere, which is shown in Figure S3 in Supporting Information S1. After the occurrence of each SKR enhancement, the intense 20 kHz NB signals were observed within 2–4 hr.

The top and bottom panels show five ENA emission enhancements with red arrows pointing to the time over which the ENA images are acquired. As shown in Figure 3, the ENA emission enhancements and the 20 kHz NB intensification are well synchronized. Almost all the captured ENA emissions are near the dawn meridian and very close to the inner magnetosphere of Saturn (6–8 R_s , 1 $R_s = 60,268$ km, between the orbits of Rhea and Dione). This is in agreement with the so-called type 2 ENA injections, which are associated with interchange instability and are often detected between about 6 and ~10 R_s (Mitchell et al., 2015). To better present the ENA emissions, the equatorial projections of the ENA are provided in the Supporting Information S1, using the algorithm developed by Bader et al. (2021), as shown in Figure S4 in Supporting Information S1. The ENA distribution corresponding to the 4th SKR intensification is slightly different, with its peak mainly concentrated between 9 and 20 R_s . However, near the dawn meridian, there is still significant ENA emission distributed in the inner magnetosphere. Figure 4a shows the variation of the 100 kHz SKR emission intensity (shown by the white dashed line above in the central panel in Figure 3). Figure 4b shows the distribution of the NB intensity at 15824 Hz in Figure 3 at different times (shown by the white dashed line below in the central panel in Figure 3). Figure 4b shows nice coherence between the dipolarization signals and the enhanced 20 kHz NB signals. Magnetic dipolarization and enhanced 20 kHz NB are strikingly consistent. The SKR enhancements have a significant time shift.

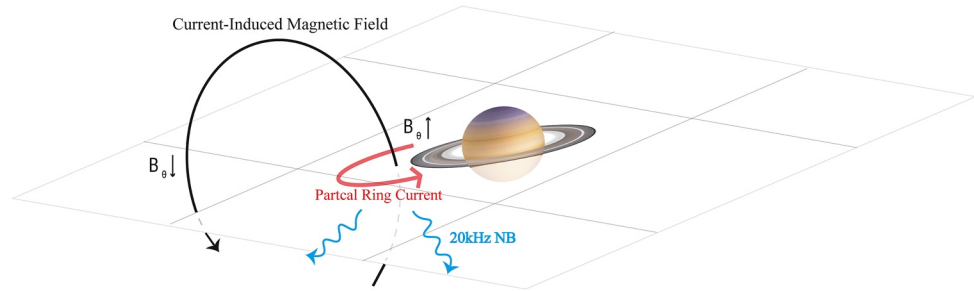
To clearly display the correlation of the magnetic dipolarization signal, SKR, 20 kHz NB and ENA emission, we collated the start/end times of all observed features in Table 1. We can see from Table 1 that the recurrent magnetic signal (B_θ rising and B_r falling, shown in Figure 1a), 20 kHz NB and ENA emission display a good correlation. The SKR enhancement shows a certain time shift, which may be due to the “hollow emission cone” propagation direction of the SKR (Galopeau et al., 1989; Zarka, 1998). SKR is emitted obliquely with respect to the magnetic field at the source and thus could be detected earlier/later.

3. Discussion and Conclusion

In this study, we made a detailed analysis of simultaneous observations of the magnetic field, electrons, ENA emissions and radio emissions using Cassini’s multiple datasets. We identified recurrent magnetic field dipolarization structures and quasi-periodic radio emissions (SKR and 20 kHz NB) over the period May 27th 00:00 to May 29th 10:00, 2009, as counterparts of the remotely sensed ENA enhancements.

At Saturn, magnetic dipolarization processes corresponding to the global current diversion can lead to global auroral enhancement (Yao, Coates, et al., 2017). In Figure 3, the ENA emission peaks and dipolarization signals are well synchronized, which implies that there is a direct connection between ENA emissions, and consequently, the underlying/parent ion distributions that produce these ENAs and magnetospheric dipolarization. The most plausible explanation for this connection may be a common current system that drives both processes, that is, an enhanced PRC, which is known to be associated with enhanced ENA emissions (Krimigis et al., 2007; Sergis et al., 2009). The increased B_θ component of the magnetic field in the region outside of the current system, characteristic of the magnetic dipolarization structures, is a manifestation of the enhanced PRC as illustrated in the schematic of Figure 5a.

a



b

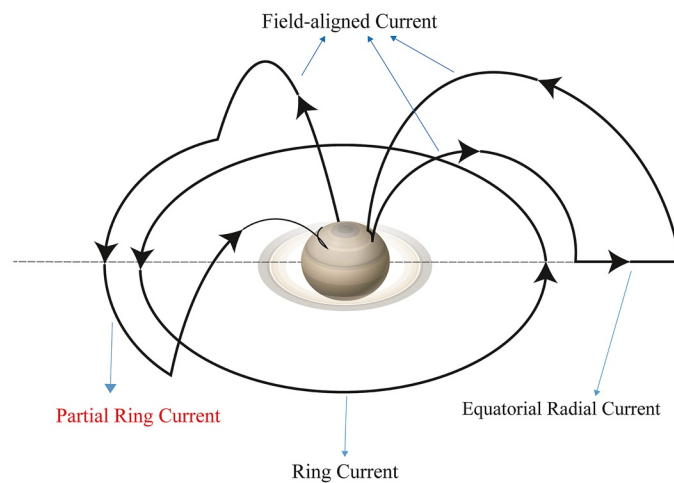


Figure 5. (a) Schematic diagram of the coupling between the inner and mid-outer magnetosphere driven by Energetic Neutral Atoms, which is applicable inside the magnetosphere. (b) A schematic of Partial Ring Current in the Saturn current system.

The current system associated with the PRC is a cutting-edge topic. Following the understanding of terrestrial PRCs (Brandt et al., 2018), we suggest the Saturnian PRCs are closed with two FAC wedges and an ionospheric electrical current jet. The distribution of Saturn's PRC in the current system is shown in Figure 5b. Although the last three detected recurrent magnetic field signals (shown in Figures 1a and 4b) are not magnetic dipolarization structures, these quasi-periodic oscillations between the cusp and polar cap were a modulation effect of the rotating PRC and associated field perturbations. Figure 6 shows the proposed picture of how PRC could affect cusp crossings. Figure 6a displays the electron energy spectrum of the observation (shown in Figure 1b) with the spacecraft position marked. Figures 6b and 6c illustrate the spacecraft's movement from its original location at low-mid latitudes within the magnetosphere to the cusp/polar cap region at high latitudes. In Figure 6d, the spacecraft's position is presented when it periodically crosses the cusp region. When PRC periodically flows by the noon side, it could cause the magnetic field within the magnetosphere to become more dipolar, which results in the cusp region being shifted up and allows Cassini to re-enter the cusp after one planetary rotation. Arridge et al. (2016) discussed that the reason the recurrent cusp observations could be the periodic oscillations in the position of Saturn's auroral oval. Given the potential link between auroral and the rotating current system (e.g., Goldreich & Farmer, 2007; Guo et al., 2021; Palmaerts et al., 2020), our proposed mechanism might offer a possible explanation for the recurrent cusp observations reported in Arridge et al. (2016). The SKR signals were also recurrent every planetary rotation, while each enhancement was shifted by a few hours with respect to the ENA (and dipolarization). The polar auroral region also emits enhanced SKR signals (Kurth et al., 2009; Lamy et al., 2008; Wu & Lee, 1979). The different phases of the SKR and ENA (and dipolarization) signals may be caused by the “hollow emission cone” of SKR (Galopeau

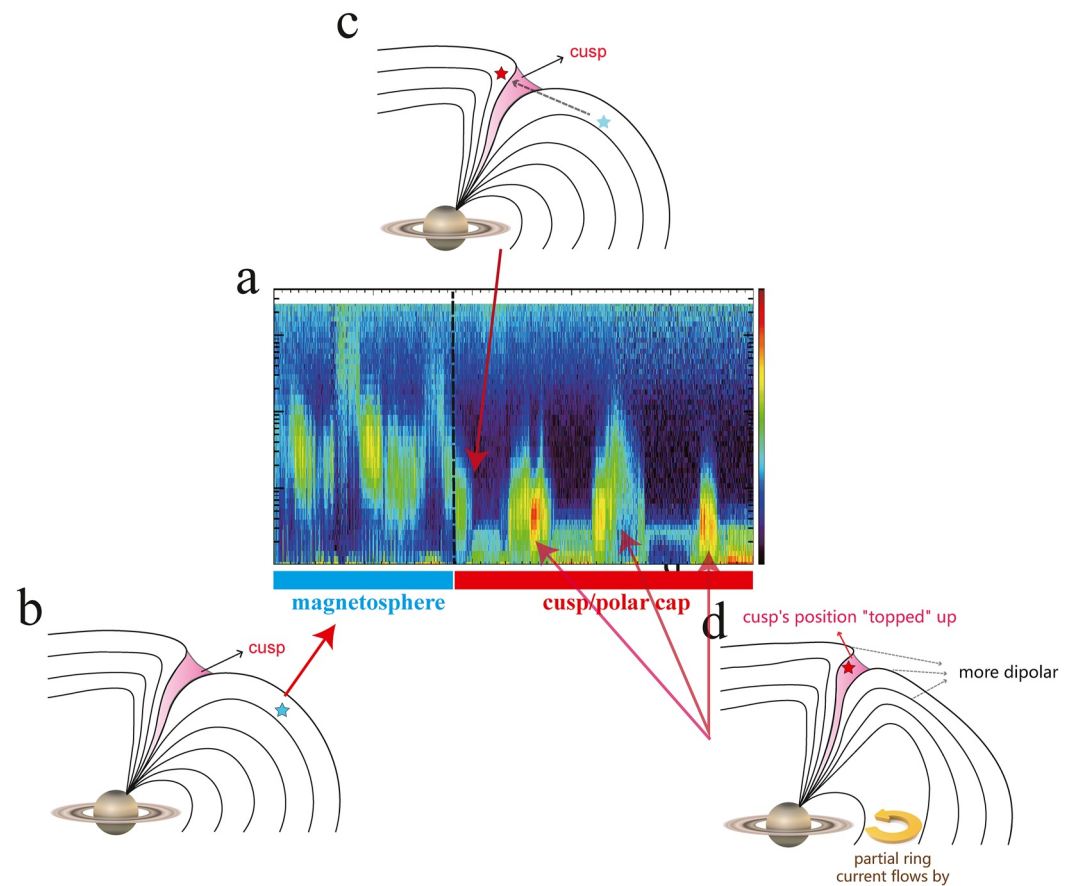


Figure 6. (a) The electron energy spectrum in Figure 1b, marked with colored bars, where the blue bar indicates that the spacecraft is in the magnetosphere and the red bar indicates that the spacecraft is in the cusp/polar cap region. (b) Schematic representation of the original location of the spacecraft during the observations with arrows pointing to the corresponding positions in panel (a). (c) Schematic of the spacecraft crossing from the magnetosphere into the polar cap/cusp region, with the arrow pointing to the corresponding position in panel (a). (d) Schematic of the spacecraft re-entering the cusp as the magnetic field becomes more dipolar when the partial ring current flows by periodically, with the arrow pointing to the corresponding position in panel (a).

et al., 1989; Zarka, 1998). SKR is emitted obliquely at the source along the magnetic field line and thus can be detected earlier/later. As shown in Table 1, if the SKR enhancement is delayed by 5 hr (perhaps due to the different beaming), its correlation with the magnetic dipolarization signal, the ENA emission and the 20 kHz NB enhancement can be clearly identified. The excitation of NB radiation is now broadly considered to include two steps in previous studies. (a) Step 1: An intense electrostatic wave is generated at a steep density gradient parallel to the magnetic field vector. (b) Step 2: The electrostatic wave is converted to an escaping electromagnetic wave via either a linear (e.g., Horne, 1989; Jones, 1976) or a nonlinear mode conversion process (e.g., Barbosa, 1982; Melrose, 1981). The steep plasma density gradient required in the first step for the generation of NB emissions can be provided by the process associated with ENA injections in the inner magnetosphere. Ye et al. (2009) had revealed that the source region of the 20 kHz NB is near the edge of the plasma torus. The Type 2 ENA injections may also generate perturbations in the inner magnetosphere (5–11 R_s) (Azari et al., 2018; Mitchell et al., 2015), thus directly affecting the plasma torus edge where the 20 kHz NB were generated. In the observations of this study, the good correlation between 20 kHz NB and ENA peaks suggests that they may be physically connected (as shown in Table 1).

In conclusion, this study proposes a unified picture that magnetic dipolarization, associated with magnetospheric current reconfiguration, appears directly coupled with enhanced ENA emissions. Both the SKR and 20 kHz NB emissions are likely linked to the enhanced ENA emission and the associated magnetospheric current reconfiguration, as manifestations of the same physical mechanism.

The main results are summarized below,

1. This study provides observational evidence of the coupling processes between ENA emission and dipolarized changes in the magnetic field structure at Saturn.
2. The 20 kHz NB emission is probably driven at the edge of plasma torus that is perturbed by ENA injections in the inner magnetosphere.
3. The magnetic dipolarization, ENA, aurora and kilometric radiations are all linked, providing new insight to understand their driving mechanisms.

Data Availability Statement

The Cassini data presented in this study are available at https://pds-ppi.igpp.ucla.edu/search/?t=Saturn&sc=Cassini&facet=SPACECRAFT_NAME&depth=1 via MAG, CAPS/ELS, MIMI, and RPWS instruments. The database of ENA projections in the Supporting Information S1 is available at <https://doi.org/10.17635/lancaster/researchdata/384> (Bader et al., 2020).

References

- Achilleos, N., Guio, P., & Arridge, C. S. (2010). A model of force balance in Saturn's magnetodisc. *Monthly Notices of the Royal Astronomical Society*, 401(4), 2349–2371. <https://doi.org/10.1111/j.1365-2966.2009.15865.x>
- Arridge, C. S., Jasinski, J. M., Achilleos, N., Bogdanova, Y. V., Bunce, E. J., Cowley, S. W., et al. (2016). Cassini observations of Saturn's southern polar cusp. *Journal of Geophysical Research: Space Physics*, 121(4), 3006–3030. <https://doi.org/10.1002/2015ja021957>
- Arridge, C. S., Russell, C. T., Khurana, K. K., Achilleos, N., Cowley, S. W. H., Dougherty, M. K., et al. (2008). Saturn's magnetodisc current sheet. *Journal of Geophysical Research*, 113(A4), A04214. <https://doi.org/10.1029/2007ja012540>
- Azari, A. R., Liemohn, M. W., Jia, X., Thomsen, M. F., Mitchell, D. G., Sergis, N., et al. (2018). Interchange injections at Saturn: Statistical survey of energetic H⁺ sudden flux intensifications. *Journal of Geophysical Research: Space Physics*, 123(6), 4692–4711. <https://doi.org/10.1029/2018ja025391>
- Bader, A., Kinrade, J., Badman, S., Paranicas, C., Constable, D., & Mitchell, D. G. (2020). Cassini INCA equatorial ENA projections [Dataset]. Lancaster University. <https://doi.org/10.17635/lancaster/researchdata/384>
- Bader, A., Kinrade, J., Badman, S. V., Paranicas, C., Constable, D. A., & Mitchell, D. G. (2021). A complete data set of equatorial projections of Saturn's energetic neutral atom emissions observed by Cassini-INCA. *Journal of Geophysical Research: Space Physics*, 126(6), e2020JA028908. <https://doi.org/10.1029/2020ja028908>
- Barbosa, D. D. (1982). Low-level VLF and LF radio emissions observed at Earth and Jupiter. *Reviews of Geophysics*, 20(2), 316. <https://doi.org/10.1029/rg020002p00316>
- Bradley, T. J., Cowley, S. W. H., Bunce, E. J., Smith, A. W., Jackman, C. M., & Provan, G. (2018). Planetary period modulation of reconnection bursts in Saturn's magnetotail. *Journal of Geophysical Research: Space Physics*, 123(11), 9476–9507. <https://doi.org/10.1029/2018ja025932>
- Brandt, P. C., Hsieh, S. Y., DeMajistre, R., & Mitchell, D. G. (2018). ENA imaging of planetary ring currents. In *Electric currents in geospace and beyond, part II: Ring currents* (pp. 95–114).
- Brandt, P. C., Khurana, K. K., Mitchell, D. G., Sergis, N., Dialynas, K., Carbary, J. F., et al. (2010). Saturn's periodic magnetic field perturbations caused by a rotating partial ring current. *Geophysical Research Letters*, 37(22), L22103. <https://doi.org/10.1029/2010gl045285>
- Brooks, E. L., Fernandez, C., & Pontius, D. H., Jr. (2019). Saturn's multiple, variable periodicities: A dual-flywheel model of thermosphere-ionosphere-magnetosphere coupling. *Journal of Geophysical Research: Space Physics*, 124(10), 7820–7836. <https://doi.org/10.1029/2019ja026870>
- Bunce, E. J., Arridge, C. S., Clarke, J. T., Coates, A. J., Cowley, S. W. H., Dougherty, M. K., et al. (2008). Origin of Saturn's aurora: Simultaneous observations by Cassini and the Hubble space telescope. *Journal of Geophysical Research*, 113(A9), A09209. <https://doi.org/10.1029/2008ja013257>
- Carbary, J. F., Krimigis, S. M., Mitchell, D. G., Paranicas, C., & Brandt, P. (2009). Energetic neutral atom (ENA) and charged particle periodicities in Saturn's magnetosphere. *Advances in Space Research*, 44(4), 483–493. <https://doi.org/10.1016/j.asr.2009.04.019>
- Carbary, J. F., & Mitchell, D. G. (2014). Keogram analysis of ENA images at Saturn. *Journal of Geophysical Research: Space Physics*, 119(3), 1771–1780. <https://doi.org/10.1002/2014ja019784>
- Carbary, J. F., Mitchell, D. G., Brandt, P., Paranicas, C., & Krimigis, S. M. (2008). ENA periodicities at Saturn. *Geophysical Research Letters*, 35(7), L07102. <https://doi.org/10.1029/2008gl033230>
- Carbary, J. F., Mitchell, D. G., Brandt, P., Roelof, E. C., & Krimigis, S. M. (2008). Statistical morphology of ENA emissions at Saturn. *Journal of Geophysical Research*, 113(A5), A05210. <https://doi.org/10.1029/2007ja012873>
- Carbary, J. F., Mitchell, D. G., Krimigis, S. M., Gurnett, D. A., & Kurth, W. S. (2010). Phase relations between energetic neutral atom intensities and kilometric radio emissions at Saturn. *Journal of Geophysical Research*, 115(A1), A01203. <https://doi.org/10.1029/2009ja014519>
- Carbary, J. F., Mitchell, D. G., Krimigis, S. M., Hamilton, D. C., & Krupp, N. (2007). Charged particle periodicities in Saturn's outer magnetosphere. *Journal of Geophysical Research*, 112(A6), A06246. <https://doi.org/10.1029/2007ja012351>
- Dialynas, K. (2018). Cassini/MIMI observations on the Dungey cycle reconnection and Kelvin-Helmholtz instability in Saturn's magnetosphere. *Journal of Geophysical Research: Space Physics*, 123(9), 7271–7275. <https://doi.org/10.1029/2018ja025840>
- Dialynas, K., Brandt, P. C., Krimigis, S. M., Mitchell, D. G., Hamilton, D. C., Krupp, N., & Rymer, A. M. (2013). The extended Saturnian neutral cloud as revealed by global ENA simulations using Cassini/MIMI measurements. *Journal of Geophysical Research: Space Physics*, 118(6), 3027–3041. <https://doi.org/10.1002/jgra.50295>
- Dialynas, K., Roussos, E., Regoli, L., Paranicas, C. P., Krimigis, S. M., Kane, M., et al. (2018). Energetic ion moments and polytropic index in Saturn's magnetosphere using Cassini/MIMI measurements: A simple model based on κ -distribution functions. *Journal of Geophysical Research: Space Physics*, 123(10), 8066–8086. <https://doi.org/10.1029/2018ja025820>

Acknowledgments

This work was supported by National Natural Science Foundation of China Grants 42074211, Key Research Program of the Institute of Geology and Geophysics, CAS, Grant IGGCAS-201904. The work at the Academy of Athens was supported at JHU/APL by NASA under contracts NAS5 97271, NNX07AJ69 G, and NNN06AA01C and by subcontract at the Office for Space Research and Technology. Work at UCL-MSSL by WD, AJC was supported by STFC Grant ST/S000240/1. Work at Lancaster was supported by STFC Grants ST/V000748/1 (SVB, JK), ST/M005534/1 (SVB), and a FST studentship (AB). Y. X. very much appreciates the fruitful discussion with Dr. Chris Arridge.

- Dougherty, M. K., Kellock, S., Southwood, D. J., Balogh, A., Smith, E. J., Tsurutani, B. T., et al. (2004). The Cassini magnetic field investigation. In *The Cassini-Huygens mission* (pp. 331–383). Springer.
- Dougherty, M. K., Khurana, K. K., Neubauer, F. M., Russell, C. T., Saur, J., Leisner, J. S., & Burton, M. E. (2006). Identification of a dynamic atmosphere at Enceladus with the Cassini magnetometer. *Science*, *311*(5766), 1406–1409. <https://doi.org/10.1126/science.1120985>
- Galopeau, P., Zarka, P., & Le Quéau, D. (1989). Theoretical model of Saturn's kilometric radiation spectrum. *Journal of Geophysical Research*, *94*(A7), 8739–8755. <https://doi.org/10.1029/ja094ia07p08739>
- Goldreich, P., & Farmer, A. J. (2007). Spontaneous axisymmetry breaking of the external magnetic field at Saturn. *Journal of Geophysical Research*, *112*(A5), A05225. <https://doi.org/10.1029/2006ja012163>
- Green, J. L., & Boardsen, S. A. (1999). Confinement of nonthermal continuum radiation to low latitudes. *Journal of Geophysical Research*, *104*(A5), 10307–10316. <https://doi.org/10.1029/1998ja900130>
- Guo, R. L., Yao, Z. H., Dunn, W. R., Palmaerts, B., Sergis, N., Grodent, D., et al. (2021). A rotating azimuthally distributed auroral current system on Saturn Revealed by the Cassini spacecraft. *The Astrophysical Journal Letters*, *919*(2), L25. <https://doi.org/10.3847/2041-8213/ac26b5>
- Gurnett, D. A. (1974). The Earth as a radio source: Terrestrial kilometric radiation. *Journal of Geophysical Research*, *79*(28), 4227–4238. <https://doi.org/10.1029/ja079i028p04227>
- Gurnett, D. A., Kurth, W. S., Kirchner, D. L., Hospodarsky, G. B., Averkamp, T. F., Zarka, P., et al. (2004). The Cassini radio and plasma wave investigation. In *The Cassini-Huygens mission* (pp. 395–463). Springer.
- Gurnett, D. A., Kurth, W. S., & Scarf, F. L. (1981). Narrowband electromagnetic emissions from Saturn's magnetosphere. *Nature*, *292*(5825), 733–737. <https://doi.org/10.1038/292733a0>
- Horne, R. B. (1989). Path-integrated growth of electrostatic waves: The generation of terrestrial myriametric radiation. *Journal of Geophysical Research*, *94*(A7), 8895. <https://doi.org/10.1029/ja094ia07p08895>
- Jackman, C. M., Lamy, L., Freeman, M. P., Zarka, P., Cecconi, B., Kurth, W. S., et al. (2009). On the character and distribution of lower-frequency radio emissions at Saturn and their relationship to substorm-like events. *Journal of Geophysical Research*, *114*(A8), A08211. <https://doi.org/10.1029/2008ja013997>
- Jaffe, L. D., & Herrell, L. M. (1997). Cassini/Huygens science instruments, spacecraft, and mission. *Journal of Spacecraft and Rockets*, *34*(4), 509–521. <https://doi.org/10.2514/2.3241>
- Jasinski, J. M., Arridge, C. S., Coates, A. J., Jones, G. H., Sergis, N., Thomsen, M. F., & Krupp, N. (2017). Diamagnetic depression observations at Saturn's magnetospheric cusp by the Cassini spacecraft. *Journal of Geophysical Research: Space Physics*, *122*(6), 6283–6303. <https://doi.org/10.1002/2016ja023738>
- Jasinski, J. M., Arridge, C. S., Coates, A. J., Jones, G. H., Sergis, N., Thomsen, M. F., et al. (2016). Cassini plasma observations of Saturn's magnetospheric cusp. *Journal of Geophysical Research: Space Physics*, *121*(12), 12–047. <https://doi.org/10.1002/2016ja023310>
- Jasinski, J. M., Arridge, C. S., Lamy, L., Leisner, J. S., Thomsen, M. F., Mitchell, D. G., et al. (2014). Cusp observation at Saturn's high-latitude magnetosphere by the Cassini spacecraft. *Geophysical Research Letters*, *41*(5), 1382–1388. <https://doi.org/10.1002/2014gl0159319>
- Jones, D. (1976). Source of terrestrial non-thermal radiation. *Nature*, *260*(5553), 686–689. <https://doi.org/10.1038/260686a0>
- Kinrade, J., Bader, A., Badman, S. V., Paranicas, C., Mitchell, D. G., Constable, D., et al. (2021). The statistical morphology of Saturn's equatorial energetic neutral atom emission. *Geophysical Research Letters*, *48*(11), e2020GL091595. <https://doi.org/10.1029/2020gl091595>
- Kinrade, J., Badman, S. V., Paranicas, C., Mitchell, D. G., Arridge, C. S., Gray, R. L., et al. (2020). Tracking counterpart signatures in Saturn's auroas and ENA imagery during large-scale plasma injection events. *Journal of Geophysical Research: Space Physics*, *125*(2), e2019JA027542. <https://doi.org/10.1029/2019ja027542>
- Kivelson, M. G. (2005). The current systems of the Jovian magnetosphere and ionosphere and predictions for Saturn. In *The outer planets and their Moons* (pp. 299–318). Springer.
- Krimigis, S. M., Mitchell, D. G., Hamilton, D. C., Krupp, N., Livi, S., Roelof, E. C., et al. (2005). Dynamics of Saturn's magnetosphere from MIMI during Cassini's orbital insertion. *Science*, *307*(5713), 1270–1273. <https://doi.org/10.1126/science.1105978>
- Krimigis, S. M., Mitchell, D. G., Hamilton, D. C., Livi, S., Dandouras, J., Jaskulek, S., et al. (2004). Magnetosphere imaging instrument (MIMI) on the Cassini mission to Saturn/Titan. In *The Cassini-Huygens mission* (pp. 233–329). Springer.
- Krimigis, S. M., Sergis, N., Mitchell, D. G., Hamilton, D. C., & Krupp, N. (2007). A dynamic, rotating ring current around Saturn. *Nature*, *450*(7172), 1050–1053. <https://doi.org/10.1038/nature06425>
- Kurth, W., Bunce, E., Clarke, J., Crary, F., Grodent, D., Ingersoll, A., et al. (2009). Auroral processes. In *Saturn from Cassini-Huygens* (pp. 333–374). Springer.
- Kurth, W. S., Gurnett, D. A., Clarke, J. T., Zarka, P., Desch, M. D., Kaiser, M. L., et al. (2005). An Earth-like correspondence between Saturn's auroral features and radio emission. *Nature*, *433*(7027), 722–725. <https://doi.org/10.1038/nature03334>
- Kurth, W. S., Gurnett, D. A., & Scarf, F. L. (1980). Spatial and temporal studies of Jovian kilometric radiation. *Geophysical Research Letters*, *7*(1), 61–64. <https://doi.org/10.1029/g1007i001p00061>
- Kurth, W. S., Hospodarsky, G. B., Gurnett, D. A., Lamy, L., Dougherty, M. K., Nichols, J., et al. (2016). Saturn kilometric radiation intensities during the Saturn auroral campaign of 2013. *Icarus*, *263*, 2–9. <https://doi.org/10.1016/j.icarus.2015.01.003>
- Lamy, L., Schippers, P., Zarka, P., Cecconi, B., Arridge, C. S., Dougherty, M. K., et al. (2010). Properties of Saturn kilometric radiation measured within its source region. *Geophysical Research Letters*, *37*(12), L12104. <https://doi.org/10.1029/2010gl043415>
- Lamy, L., Zarka, P., Cecconi, B., Prangé, R., Kurth, W. S., & Gurnett, D. A. (2008). Saturn kilometric radiation: Average and statistical properties. *Journal of Geophysical Research*, *113*(A7), A07201. <https://doi.org/10.1029/2007ja012900>
- Lamy, L., Zarka, P., Cecconi, B., Prangé, R., Kurth, W. S., Hospodarsky, G., et al. (2018). The low-frequency source of Saturn's kilometric radiation. *Science*, *362*(6410), eaat2027. <https://doi.org/10.1126/science.aat2027>
- Melrose, D. B. (1981). A theory for the nonthermal radio continua in the terrestrial and Jovian magnetospheres. *Journal of Geophysical Research*, *86*(A1), 30–36. <https://doi.org/10.1029/ja086ia01p00030>
- Mitchell, D. G., Brandt, P. C., Carbary, J. F., Kurth, W. S., Krimigis, S. M., Paranicas, C., et al. (2015). Injection, interchange, and reconnection: Energetic particle observations in Saturn's magnetosphere. *Magnetotails in the Solar System*, 327–343. <https://doi.org/10.1002/9781118842324.ch19>
- Mitchell, D. G., Krimigis, S. M., Paranicas, C., Brandt, P. C., Carbary, J. F., Roelof, E. C., et al. (2009). Recurrent energization of plasma in the midnight-to-dawn quadrant of Saturn's magnetosphere, and its relationship to auroral UV and radio emissions. *Planetary and Space Science*, *57*(14–15), 1732–1742. <https://doi.org/10.1016/j.pss.2009.04.002>
- Mitchell, D. G., Kurth, W. S., Hospodarsky, G. B., Krupp, N., Saur, J., Mauk, B. H., et al. (2009). Ion conics and electron beams associated with auroral processes on Saturn. *Journal of Geophysical Research*, *114*(A2), A02212. <https://doi.org/10.1029/2008ja013621>
- Morgan, D. D., & Gurnett, D. A. (1991). The source location and beaming of terrestrial continuum radiation. *Journal of Geophysical Research*, *96*(A6), 9595–9613. <https://doi.org/10.1029/91ja00314>

- Palmaerts, B., Yao, Z. H., Sergis, N., Guo, R. L., Grodent, D., Dialynas, K., et al. (2020). A long-lasting auroral spiral rotating around Saturn's pole. *Geophysical Research Letters*, *47*(23), e2020GL088810. <https://doi.org/10.1029/2020gl088810>
- Schippers, P., André, N., Gurnett, D. A., Lewis, G. R., Persoon, A. M., & Coates, A. J. (2012). Identification of electron field-aligned current systems in Saturn's magnetosphere. *Journal of Geophysical Research*, *117*(A5), A05204. <https://doi.org/10.1029/2011ja017352>
- Sergis, N., Jackman, C. M., Thomsen, M. F., Krimigis, S. M., Mitchell, D. G., Hamilton, D. C., et al. (2017). Radial and local time structure of the Saturnian ring current, revealed by Cassini. *Journal of Geophysical Research: Space Physics*, *122*(2), 1803–1815. <https://doi.org/10.1002/2016ja023742>
- Sergis, N., Krimigis, S. M., Mitchell, D. G., Hamilton, D. C., Krupp, N., Mauk, B. H., et al. (2009). Energetic particle pressure in Saturn's magnetosphere measured with the magnetospheric imaging instrument on Cassini. *Journal of Geophysical Research*, *114*(A2), A02214. <https://doi.org/10.1029/2008ja013774>
- Sergis, N., Krimigis, S. M., Mitchell, D. G., Hamilton, D. C., Krupp, N., Mauk, B. M., et al. (2007). Ring current at Saturn: Energetic particle pressure in Saturn's equatorial magnetosphere measured with Cassini/MIMI. *Geophysical Research Letters*, *34*(9), L09102. <https://doi.org/10.1029/2006gl029223>
- Smith, H. T., Johnson, R. E., Perry, M. E., Mitchell, D. G., McNutt, R. L., & Young, D. T. (2010). Enceladus plume variability and the neutral gas densities in Saturn's magnetosphere. *Journal of Geophysical Research*, *115*(A10), A10252. <https://doi.org/10.1029/2009ja015184>
- Wing, S., Brandt, P. C., Mitchell, D. G., Johnson, J. R., Kurth, W. S., & Menietti, J. D. (2020). Periodic narrowband radio wave emissions and inward plasma transport at Saturn's magnetosphere. *The Astronomical Journal*, *159*(6), 249. <https://doi.org/10.3847/1538-3881/ab818d>
- Wu, C. S., & Lee, L. C. (1979). A theory of the terrestrial kilometric radiation. *The Astrophysical Journal*, *230*, 621–626. <https://doi.org/10.1086/157120>
- Yao, Z. (2017). Observations of loading-unloading process at Saturn's distant magnetotail. *Earth and Planetary Physics*, *1*(1), 53–57. <https://doi.org/10.26464/epp2017007>
- Yao, Z. H., Coates, A. J., Ray, L. C., Rae, I. J., Grodent, D., Jones, G. H., et al. (2017). Corotating magnetic reconnection site in Saturn's magnetosphere. *The Astrophysical Journal Letters*, *846*(2), L25. <https://doi.org/10.3847/2041-8213/aa88af>
- Yao, Z. H., Grodent, D., Ray, L. C., Rae, I. J., Coates, A. J., Pu, Z. Y., et al. (2017). Two fundamentally different drivers of dipolarizations at Saturn. *Journal of Geophysical Research: Space Physics*, *122*(4), 4348–4356. <https://doi.org/10.1002/2017ja024060>
- Yao, Z. H., Radioti, A., Grodent, D., Ray, L. C., Palmaerts, B., Sergis, N., et al. (2018). Recurrent magnetic dipolarization at Saturn: Revealed by Cassini. *Journal of Geophysical Research: Space Physics*, *123*(10), 8502–8517. <https://doi.org/10.1029/2018ja025837>
- Ye, S. Y., Gurnett, D. A., Fischer, G., Cecconi, B., Menietti, J. D., Kurth, W. S., et al. (2009). Source locations of narrowband radio emissions detected at Saturn. *Journal of Geophysical Research*, *114*(A6), A06219. <https://doi.org/10.1029/2008ja013855>
- Young, D. T., Berthelier, J. J., Blanc, M., Burch, J. L., Coates, A. J., Goldstein, R., et al. (2004). Cassini plasma spectrometer investigation. In *The Cassini-Huygens mission* (pp. 1–112). Springer.
- Zarka, P. (1998). Auroral radio emissions at the outer planets: Observations and theories. *Journal of Geophysical Research*, *103*(E9), 20159–20194. <https://doi.org/10.1029/98je01323>